

VALORIZATION OF COBALT FROM WASTE LIB CATHODE THROUGH COBALT OXALATE AND COBALT OXIDE SYNTHESIS BY LEACHING-SOLVENT EXTRACT-PRECIPITATION STRIPPING

An ecoefficient, economical and sustainable valorization process for the synthesis of Co_3O_4 from waste lithium-ion battery (LIB) by leaching-solvent extract-scrubbing-precipitation stripping route has been developed. Through an optimization, the waste LIB cathode was leached using 2000 mole/ m^3 of H_2SO_4 and 5 Vol. % of the H_2O_2 at a pulp density of 100 kg/m^3 under leaching time 60 minutes and temperature 75 °C. From the separated leach liquor, cobalt was purified by saponified Cyanex 272. From cobalt, loaded Cyanex 272 impurities were scrubbed and the $\text{CoC}_2\text{O}_4 \cdot 2\text{H}_2\text{O}$ was recovered through precipitation stripping. Finally, the precipitate was calcined to synthesize Co_3O_4 , which is a precursor for LIB cathode materials manufacturing. From TGA-DTA, followed by XRD analysis it was confirmed that at 200 °C the $\text{CoC}_2\text{O}_4 \cdot 2\text{H}_2\text{O}$ can be converted to anhydrous CoC_2O_4 and at 350 °C the anhydrous can be converted to Co_3O_4 and at 1100 °C the Co_3O_4 can be converted to CoO. Through reported route waste LIB can back to LIB manufacturing process through a versatile and flexible industrial approach.

Keywords: Valorization of cobalt, Cobalt oxide powder, Rod-shaped cobalt oxalate, Precipitation stripping

1. Introduction

Numerous author has been reported metal value recovery from waste lithium-ion battery (LIB), also several industries around the world recycling waste LIB for recovery of metal values [1-3]. Despite cobalt is not a rare metal but consider as a critical metal because of its availability and geopolitical issues. Hence, recycling of LIB being conducted around the world for recovery of cobalt from this secondary resources to keep a stable supply, circularize economy and addresses issues like; environment, landfilling, WEEE directives, and other stringent environment directives. Cobalt essentially is critical metal for LIB, and currently 42% of global cobalt production used for the battery manufacturing. Marketandmarkets research Pvt. Ltd. has predicted the LIB market is expected to reach USD 68.97 billion by 2022, growing at a CAGR of 16.6% between 2016 and 2022 [4]. Cobalt oxides (Co_3O_4) for battery production being commonly used as precursors for the battery cathode materials for LIB and lithium polymer batteries. Because of pure Co_3O_4 nanopowder possess superior properties like; electrochemical, electrical, magnetic, and superior catalytic effects, compared to bulk Co_3O_4 , the Co_3O_4 nanopowder used as electrode active materials or battery material. The Co_3O_4 nanopowder not only used for LIB manufacturing, but also as catalyst, superconductors, electronic ceramics, and industrial oxidant. Various shaped Co_3O_4 , i.e., nanotubes, na-

norods, and nanoparticles are used as precursor materials for LIB manufacturing [5-7].

In the literature, several Co_3O_4 synthesis methods like oxidation-reduction [8], hydrothermal synthesis [9,10], thermal decomposition [11], (co)precipitation [12] and the sol-gel [13] have been reported. Most of the Co_3O_4 synthesis method uses mainly pure and expensive chemical resources. Although numerous studies are reported, there is very inadequate connection between research on Co_3O_4 nanopowder synthesis and industrial process for mass production. Mass production of industrial grade Co_3O_4 by the above-mentioned methods associated with several challenges; expensive instrumentation, specialized facilities, high volume of precursor consumption, energy-intensive process, greater environmental risk, and occupational safety [14]. Waste LIB is successfully used as secondary resources for cobalt recovery and Co_3O_4 being synthesized from pure chemical, which are essentially two different processes subject to two different industrial processes involvement. Valorization of waste LIB through the synthesis of LIB precursor Co_3O_4 direct from waste LIB back to LIB manufacturing process is scarce. Our current valorization process combines LIB recycling process and synthesis of Co_3O_4 together which eliminate the pure cobalt recovery process and preliminary processes for the synthesis of LIB precursor (Co_3O_4) material. More importantly, it can be industrially feasible valorization process capable of mass

* ADVANCED MATERIALS & PROCESSING CENTER, INSTITUTE FOR ADVANCED ENGINEERING (IAE), YONGIN, REPUBLIC OF KOREA

** MINERAL RESOURCES RESEARCH DIVISION, KOREA INSTITUTE OF GEOSCIENCE AND MINERAL RESOURCES (KIGAM), DAEJEON 305-350, REPUBLIC OF KOREA

[#] Corresponding author: cglee@iae.re.kr, swain@iae.re.kr

production of LIB precursor (Co_3O_4) material from waste LIB cathode through the simplest leaching-solvent extract-scrubbing-precipitation stripping process. The importance and novelty of the reported process explained below.

- 1) Most of the Co_3O_4 synthesis reported literature is from the pure chemical precursor, whereas in our current method, the waste LIB cathode is used as the resources material. Through leaching-solvent extract-precipitation stripping, pure hydrated cobalt oxalate ($\text{CoC}_2\text{O}_4 \cdot 2\text{H}_2\text{O}$) was recovered followed by, the Co_3O_4 was synthesized through simple calcination.
- 2) Most of the Co_3O_4 synthesis described in the literature is about a gram to sub-gram material synthesis process, but our process offers a versatile and flexible approach for mass production capability up to kilogram scale. Unlike reported process, the valorization process can be a continuous process instead of batch process.
- 3) The developed Co_3O_4 synthesis process is a sustainable, ecoefficient, techno-economical feasible processes for commercial production of Co_3O_4 powder.

2. Materials and method

All chemicals like H_2SO_4 , H_2O_2 , Na_2CO_3 , oxalic acid ($\text{C}_2\text{H}_2\text{O}_4$) (Junsei Chemical Co., Japan) were of analytical grade (A.R.) reagent. The extractant Cyanex 272 was supplied by Cytec Korea, Inc. was used without further purification. The low boiling point kerosene (180-270 °C) was used as a diluent and TBP (Tri-*n*-butyl-phosphate) was used as phase modifier. Cobalt

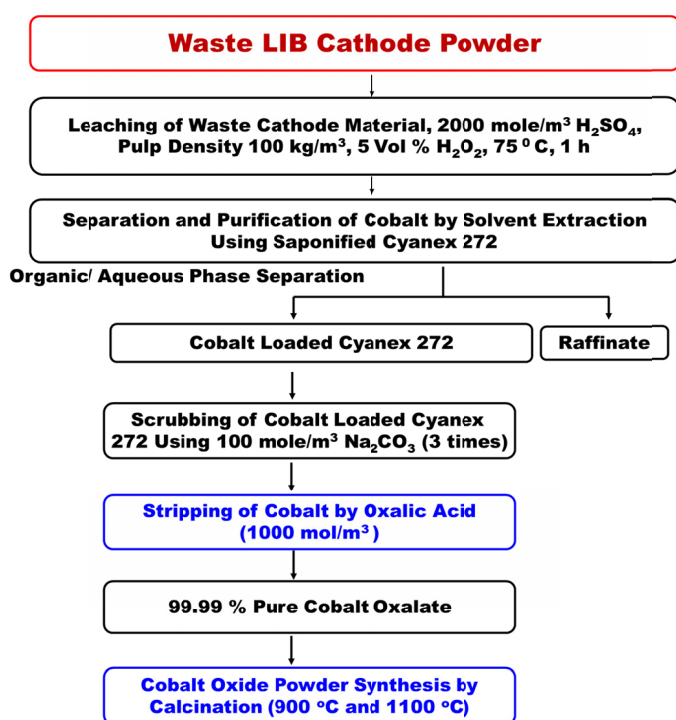


Fig. 1. The process flow sheet for the cobalt recovery, purification, and synthesis of cobalt oxalate powder by precipitation stripping from purified cobalt

from waste LIB cathode has been purified by the hydrometallurgical process reported elsewhere [15]. The process flow sheet depicted in Fig. 1. Figure 1 represents the leaching of cobalt from waste LIB, purification of cobalt by solvent extraction, and precipitation stripping of hydrated $\text{CoC}_2\text{O}_4 \cdot 2\text{H}_2\text{O}$ powder by hydrometallurgical route. From the hydrated $\text{CoC}_2\text{O}_4 \cdot 2\text{H}_2\text{O}$ precipitate, the Co_3O_4 was synthesized by calcination.

The concentration of lithium in leach liquor, raffinate, and stripped solution were determined using atomic absorption spectrometry (AAS) after dilution of the samples with 5 Vol % of HCl. The concentrations in the organic phases were determined by mass balance calculation method. AAS Varian spectra-400 was used for the analysis of metal in aqueous solutions. The maximum deviations were permitted were about $\pm 5\%$. The crystalline phase of the synthesized CoC_2O_4 , Co_3O_4 and CoO powders were characterized by X-ray diffraction (XRD), using Cu-K α radiation (RTP 300RC, Rigaku, Japan) and morphology of synthesized powder were analyzed field emission scanning electron microscopy (FE-SEM, JEM-6380LA, JEOL, Japan). Thermogravimetric analysis (TGA) and differential thermal analysis (DTA) were performed using the DTA-50 and TGA-50 devices (TA 50WSI, Shimadzu) at a heating rate of 1 °C/min for the synthesized powder.

3. Result and discussion

3.1. Characterization of waste LIB cathode powder

The XRD patterns, particle size, and SEM image for waste LIB cathode powder were analyzed and presented in Fig. 2a-c, respectively. The XRD pattern for waste LIB cathode powder shown in Fig. 2a indicated that the waste is LiCoO_2 . Fig. 2b shows the average particle size was about 8.26 μm . SEM from Fig. 2c indicated that the waste LIB cathode powder is irregular shaped with very limited agglomeration. The limited agglomeration appeared in the SEM may be due to the presence of binder in the waste LIB cathode powder. The structure and texture indicated that it could be safely leached without further treatment. Followed by characterization the waste material was leached to extract the cobalt into the acid solution from solid LiCoO_2 powder.

3.2. Purification of cobalt from waste LIB cathode by hydrometallurgy

As reported elsewhere [1], leaching optimization indicated 93% of cobalt and 94% of lithium can be leached under optimized experimental condition i.e., pulp density 100 kg/m^3 under leaching time 1 h and temperature 75 °C. Total $1 \times 10^{-3} \text{ m}^3$ of leach liquor was produced by leaching of waste LIB cathode material through 4 batches, at the optimum condition. All batches leaching experiments were conducted in a $0.5 \times 10^{-3} \text{ m}^3$ three-necked, round-bottomed pyrex reactor under controlled temperature. The

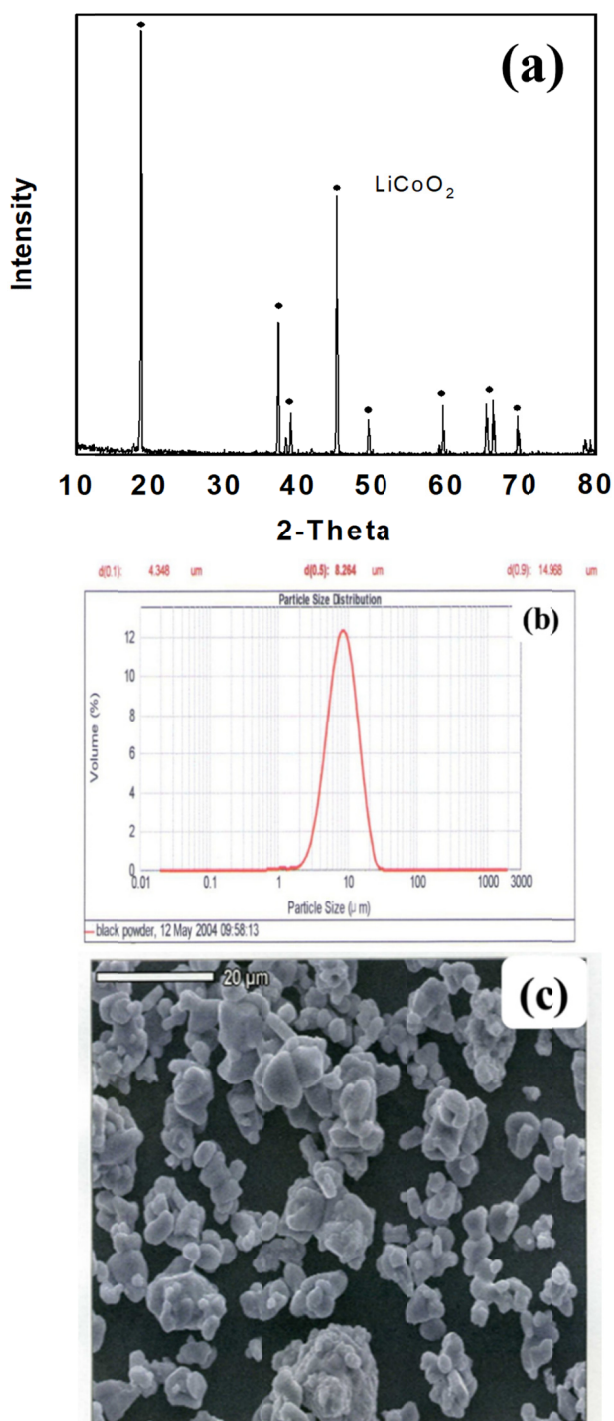


Fig. 2. (a) XRD patterns, (b) particle size, and (c) SEM image for waste LIB cathode material

reactor was fitted with an impeller stirrer, a reflux condenser, and thermometer and is described elsewhere [16]. The 2000 mole/m³ (0.25 × 10⁻³ m³) of H₂SO₄ was poured into the reactor and allowed to reach thermal equilibrium, then the measured amount of waste LIB cathode powder and 5 Vol. % of H₂O₂ solution were added into the reactor with agitating by an impeller stirrer. The leach liquor generated under optimum condition contains 44.72 kg/m³ cobalt and 5.43 kg/m³ lithium. This leach liquor was used for further purification of cobalt by solvent extraction using Cyanex 272 as an extractant.

The extractant Cyanex 272 (1000 mole/m³) was saponified up to 65% using concentrated NaOH and 5 Vol. % (TBP) was used as phase modifier. The 65% saponified Cyanex 272 was equilibrated with the leach liquor at pH 5.00 with an O/A ratio of 2 for 10 minutes. The requisite pH of the aqueous leach liquor feed was adjusted using NaOH. Followed by equilibrium the phase separation was achieved within 5 minutes, and both phases were separated. The aqueous raffinate was analyzed to determine the amount of cobalt and lithium extracted by organic extractant. The analysis indicated 78.75% of cobalt extracted from leach liquor, which corresponds to 17.61 kg/m³ cobalt loading in the organic phase. Similarly, the 13.81% lithium was co-extracted corresponds to 0.38 kg/m³ extraction into the organic phase. For further purification of cobalt, the lithium was scrubbed using 100 mole/m³ Na₂CO₃ solution (three times) at an O/A=0.5. During scrubbing 0.1 kg/m³ of cobalt and 0.09 kg/m³ lithium was scrubbed out in each stage. From this purified cobalt loaded-organic solvent, hydrated CoC₂O₄·2H₂O was synthesized through precipitation stripping.

3.3. Synthesis of cobalt oxalate and cobalt oxide powder by precipitation stripping

The purified cobalt loaded organic was stripped using 1000 mole/m³ of oxalic acid. In presence of oxalic acid (C₂H₂O₄), hydrated CoC₂O₄·2H₂O was precipitated out. The precipitate was centrifuged at 5000 rpm for 10 minutes. After centrifugation, the hydrated CoC₂O₄·2H₂O precipitate was separated from the organic phase, and the hydrated CoC₂O₄·2H₂O precipitate was acetone washed for removal of the organic extractant. The precipitate was dried in an oven at 90 °C for overnight. The dried CoC₂O₄·2H₂O was characterized by TG-DTA, XRD, and SEM. Fig. 3 shows TG-DTA curve for the dry cobalt oxalate precipitate sample. TGA for oxalate shows three different transitions at 223 °C, 360 °C, and 808 °C which corresponds to the conversion of CoC₂O₄·2H₂O to CoC₂O₄, CoC₂O₄ to Co₃O₄, Co₃O₄ to CoO, respectively. In the same figure, the DTA curve shows two different endothermic trough and exothermic peak at 200 °C and 364 °C, respectively. The endothermic trough started at 163 °C, reached to bottom at 200 °C and reverse at 223 °C, which corresponds to 19.21% of weight loss. The weight loss CoC₂O₄·2H₂O to CoC₂O₄, calculated to be 19.69% which is matching to endothermic trough in DTA curve and weight loss transition in TGA curve at 200 °C, hence, concluded conversion of CoC₂O₄·2H₂O to CoC₂O₄ at 200-223 °C. Similarly, the exothermic peak reached to maxima at 364 °C, which corresponds to 41.77% of weight loss in TGA curve against the theoretical weight loss for conversion CoC₂O₄ to Co₃O₄ 45.38%. Reasonably, it can be concluded that the transition in TGA-curve at 364 °C is due to conversion of CoC₂O₄ to Co₃O₄. The conversion of CoC₂O₄ to Co₃O₄ was further confirmed by XRD analysis through calcination at 360 °C. The DTA indicated the conversion CoC₂O₄·2H₂O to CoC₂O₄ is an endothermic reaction and conversion CoC₂O₄ to the Co₃O₄ is an exothermic reaction. Fig. 4 shows XRD pattern and SEM

of hydrated $\text{CoC}_2\text{O}_4 \cdot 2\text{H}_2\text{O}$ isolated/recovered/purified through precipitation stripping. XRD pattern in the Fig. 4a confirmed the precipitated sample is single phased $\text{CoC}_2\text{O}_4 \cdot \text{H}_2\text{O}$ powder (JCPDS#01-0296-cobalt oxalate hydrate). Morphology analysis through the SEM image in the Fig. 4b shows the precipitated has rod-like structure. Hence, rod-shaped $\text{CoC}_2\text{O}_4 \cdot \text{H}_2\text{O}$ was synthesized through the proposed process.

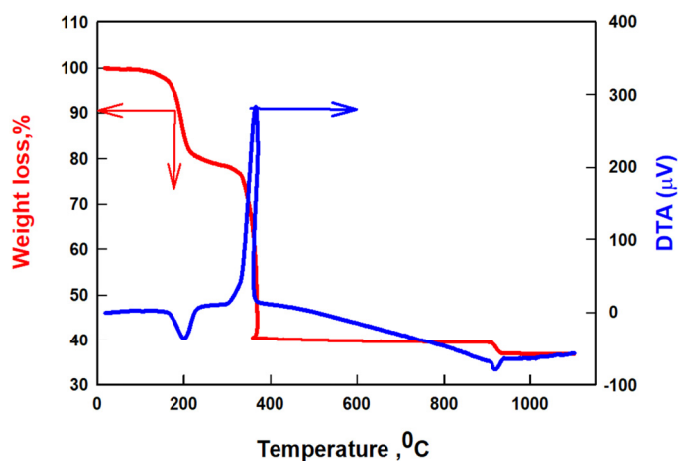


Fig. 3. TG-DTA of dry cobalt oxalate precipitate

For better understanding, based on TGA-DTA characterization, samples were synthesized by calcination at 100, 200, 250, 360, 450, 900, and 1100 °C. The XRD pattern of all the synthesized sample was analyzed and presented in Fig. 5. The XRD pattern clearly indicated up to 200 °C the synthesized cobalt oxalate remained as hydrated $\text{CoC}_2\text{O}_4 \cdot 2\text{H}_2\text{O}$ (JCPDS#01-0296-cobalt oxalate hydrate) and at 250 °C the hydrated $\text{CoC}_2\text{O}_4 \cdot 2\text{H}_2\text{O}$ converted to anhydrous CoC_2O_4 . The diffraction peaks appeared around $2\theta = 18.8^\circ, 31.1^\circ, 36.6^\circ, 38.3^\circ, 44.6^\circ, 55.5^\circ, 59.1^\circ$ and 65.0° for the calcined sample at 900, 450, and 360 °C can be assigned to 111, 220, 311, 222, 400, 422, 511, 440 planes, respectively, indicated cubic spinel structure (JCPDS# 43-1003) for Co_3O_4 . The XRD pattern for the calcined sample at 360 °C confirmed the synthesis Co_3O_4 in the cubic spinel structure (JCPDS# 43-1003). As TGA curve indicated, the calcined sample at 450, 900 °C confirmed to be well-crystallized Co_3O_4 in the cubic spinel structure (JCPDS# 43-1003). Luisetto et al. also reported a similar pattern of XRD for the synthesis of Co_3O_4 from $\text{CoC}_2\text{O}_4 \cdot \text{H}_2\text{O}$ powder[17]. The comparison of XRD pattern in the Fig. 5 for the calcined sample at 360, 450, and 900 °C indicated crystallinity of Co_3O_4 get clearer and well defined at a higher temperature of calcination (450, and 900 °C). The XRD pattern comparison of the calcined sample at 250, and 360 °C indicated decomposition of CoC_2O_4 to Co_3O_4 ; Mohameda et al. also reported similar thermal reactivity[18]. The same figure also indicated that the calcined sample at 1100 °C has diffraction peaks appeared at $2\theta = 36.6^\circ, 42.2^\circ, 61.3^\circ, 73.7^\circ$ and 77.2° were assigned to 111, 200, 220, 311, 222 planes, respectively are replications of cubic phase CoO (JCPDS # 43-1004). The XRD pattern comparison in Fig. 5 supports the conclusions made based on TGA-DTA curve when samples were selectively calcined

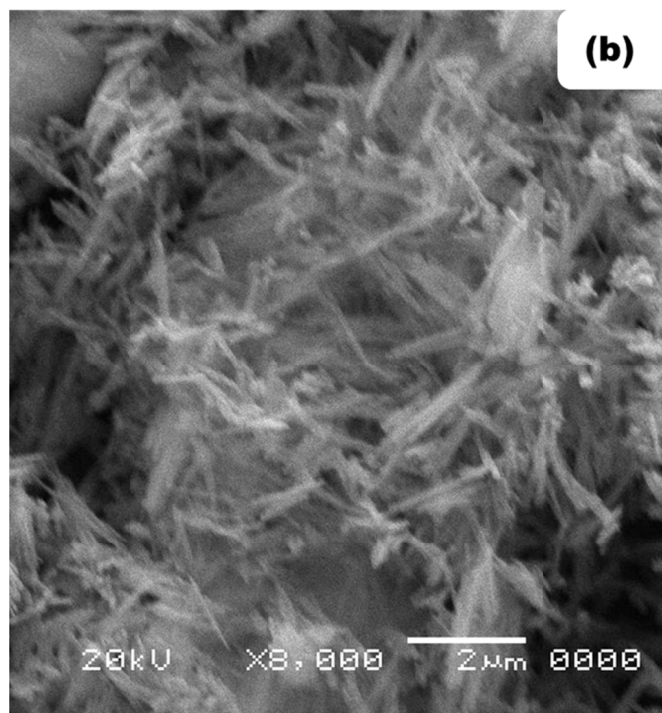
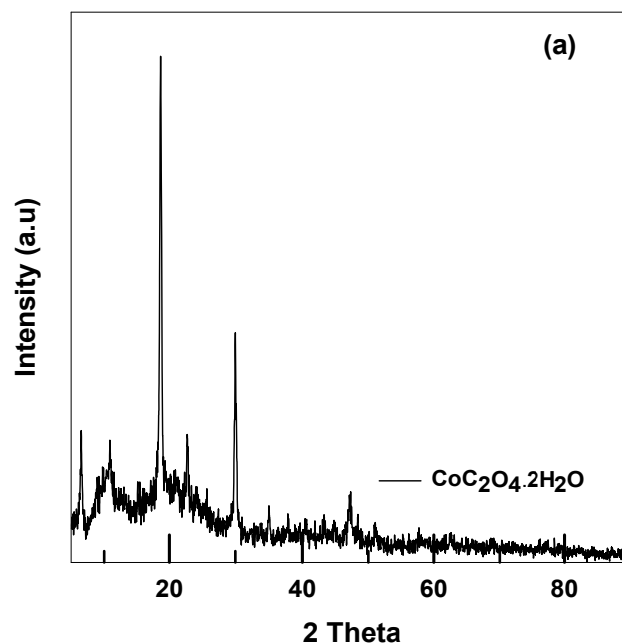


Fig. 4. (a) XRD pattern and (b) SEM image of precipitation stripped hydrated $\text{CoC}_2\text{O}_4 \cdot 2\text{H}_2\text{O}$ precipitate sample

at 100, 200, 250, 360, 450, 900, and 1100 °C, respectively. At 360 °C the anhydrous CoC_2O_4 converted to Co_3O_4 and the Co_3O_4 converted to CoO at 1100 °C. Fig. 6 represents SEM micrograph of two selective powder, i.e., CoC_2O_4 and Co_3O_4 synthesized at 250 and 450 °C, respectively. The figure clearly shows rod-shaped CoC_2O_4 powdered can be conveniently synthesized from waste LIB. From the CoC_2O_4 powder, Co_3O_4 rod-shaped powder can be synthesized. The synthesis process can close the loop; the cobalt recovered from waste LIB cathode material can valorize through rod-shaped Co_3O_4 powder synthesis and bring back for battery manufacturing as a precursor for LIB manufacturing.

XRD pattern for precipitate at different temperature

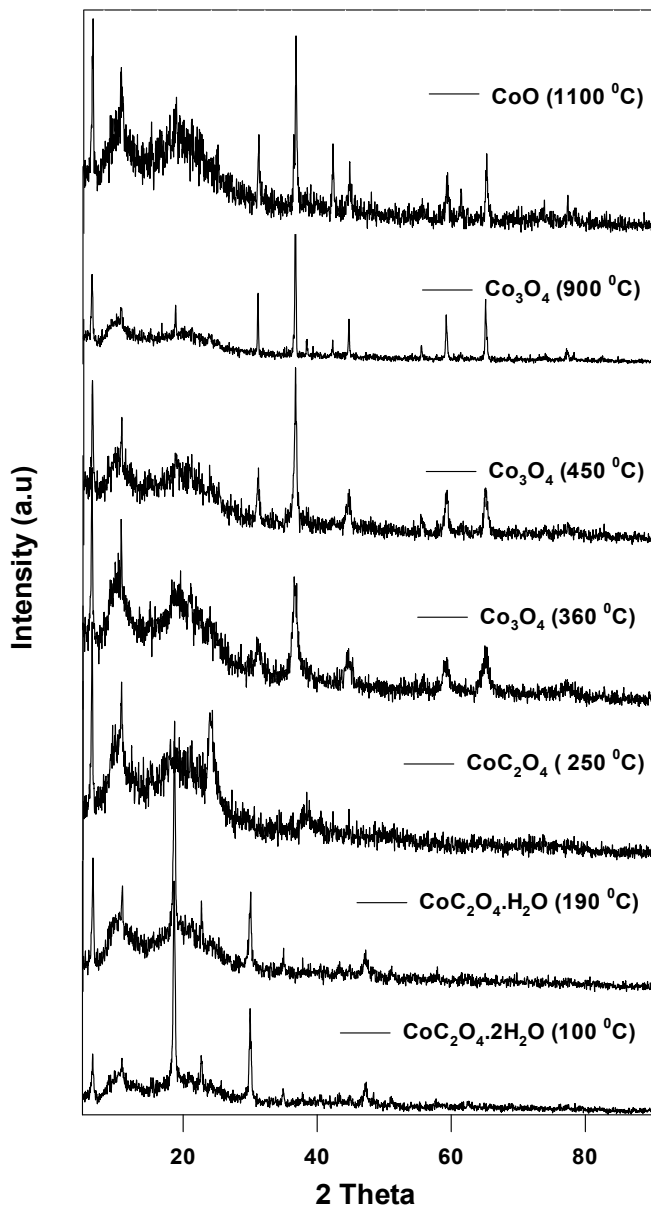


Fig. 5. XRD pattern of pure CoC_2O_4 sample calcined at 100, 200, 250, 360, 450, 900, and 1100 °C

4. Conclusion

Instead of the pure chemical precursor, from a complex and impure LIB waste cathode, the value added rod-shaped CoC_2O_4 and the Co_3O_4 powder was synthesized, which is an industrially feasible, ecoefficient, economical and sustainable process. Valorization of waste LIB through selective purification cobalt by solvent extraction and technique for the synthesis of pure rod-shaped Co_3O_4 powder has been achieved. The technique can be a versatility and flexibility process for mass production of pure CoC_2O_4 and Co_3O_4 powder. The developed cobalt powder recovery process reported can synthesize rod-shaped pure Co_3O_4 powder in the range of 1 μm size from the reported one-pot synthesis through simple precipitation stripping. Even

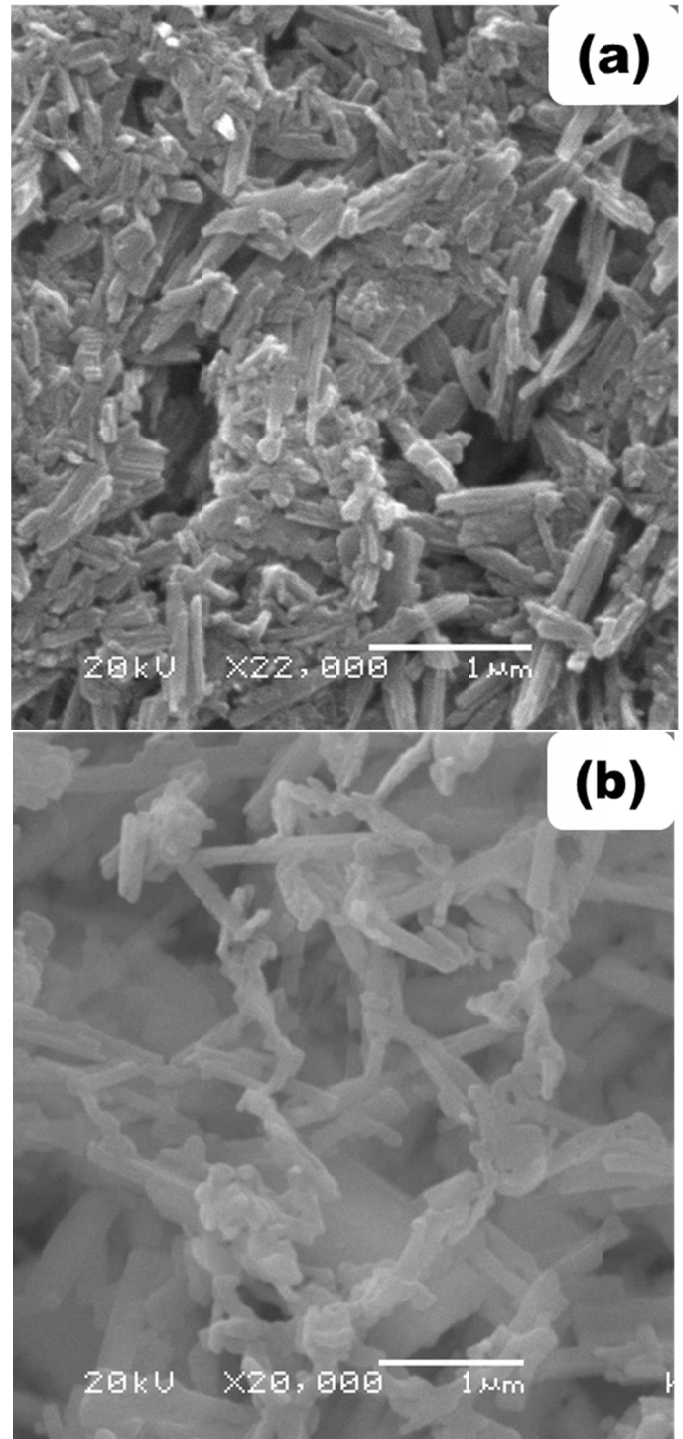


Fig. 6. SEM image of (a) CoC_2O_4 powder and (b) Co_3O_4 powder synthesized at 250 and 450 °C, respectively

in the existing LIB recycling industry can mass-produce pure CoC_2O_4 and Co_3O_4 powder by simple addition of a reactor for precipitation stripping of hydrated $\text{CoC}_2\text{O}_4 \cdot 2\text{H}_2\text{O}$, which can add values for existing industry. As the process reported is a simple process, do not require any special industrial facilities, through which waste LIB recycling industry can produce pure CoC_2O_4 and Co_3O_4 powder. The reported technique can be supplemented in the existing waste LIB cathode recycling industry for valorization waste LIB cathode material.

REFERENCES

- [1] B. Swain, J. Jeong, J.-C Lee, G.-H. Lee, J.-S. Sohn, *Journal of Power Sources* **167**, 536-544 (2007).
- [2] P. Zhang, T. Yokoyama, O. Itabashi, T. M. Suzuki, K. Inoue, *Hydrometallurgy* **47**, 259-271 (1998).
- [3] X. Chen, C. Luo, J. Zhang, J. Kong, T. Zhou, *ACS Sustainable Chemistry & Engineering* **3**, 3104-3113 (2015).
- [4] <http://www.marketsandmarkets.com> lithium Ion Battery Market worth 68.97 Billion USD by 2022 <http://www.marketsandmarkets.com/PressReleases/lithium-ion-battery.asp> (2017).
- [5] W.Y. Li, L.N. Xu, J. Chen, *Advanced Functional Materials* **15**, 851-857 (2005).
- [6] X.W. Lou, D. Deng, J.Y. Lee, J. Feng, L.A. Archer, *Advanced Materials* **20**, 258-262 (2008).
- [7] S.K. Meher, G.R. Rao, *The Journal of Physical Chemistry C* **115**, 15646-15654 (2011).
- [8] T. Ozkaya, A. Baykal, Y. Koseoğlu, H. Kavas, *Open Chemistry* **7** (2009).
- [9] L. Jin, X. Li, H. Ming, H. Wang, Z. Jia, Y. Fu, J. Adkins, Q. Zhou, J. Zheng, *RSC Advances* **4**, 6083-6089 (2014).
- [10] C.J. Denis, C.J. Tighe, R.I. Gruar, N.M. Makwana, J.A. Darr, *Crystal Growth & Design* **15**, 4256-4265 (2015).
- [11] J.K. Sharma, P. Srivastava, G. Singh, M.S. Akhtar, S. Ameen, *Materials Science and Engineering: B* **193**, 181-188 (2015).
- [12] H. Xu, J.-X. Zhuang, J.-L. Li, J.-L. Zhang, H.-L. Lu, *Ionics* **20**, 489-494 (2014).
- [13] K. Sinkó, G. Szabó, M. Zrínyi, *Journal of Nanoscience and Nanotechnology* **11**, 4127-4135 (2011).
- [14] F. Yilmaz, D.-J. Lee, J.-W. Song, H.-S. Hong, H.-T. Son, J.-S. Yoon, S.-J. Hong, *Powder Technology* **235**, 1047-1052 (2013).
- [15] B. Swain, *Journal of Chemical Technology & Biotechnology* (2017).
- [16] B. Swain, C. Mishra, L. Kang, K.-S. Park, C.G. Lee, H.S. Hong, J.-J. Park, *Journal of Power Sources* **281**, 265-271 (2015).
- [17] I. Luisetto, F. Pepe, E. Bemporad, *Journal of Nanoparticle Research* **10**, 59-67 (2008).
- [18] M.A. Mohamed, A.K. Galwey, S.A. Halawy, *Thermochimica Acta* **429**, 57-72 (2005).